Int J Earth Sci (Geol Rundsch) (2005) 94: 231–242
DOI 10.1007/s00531-005-0464-5

ORIGINAL PAPER

Marc Polliand · Urs Schaltegger · Martin Frank
Lluis Fontboté

Formation of intra-arc volcanosedimentary basins in the western flank of the central Peruvian Andes during Late Cretaceous oblique subduction: field evidence and constraints from U–Pb ages and Hf isotopes

Received: 16 October 2003 / Accepted: 11 December 2004 / Published online: 16 February 2005

Abstract During late Early to Late Cretaceous, the Peruvian coastal margin underwent fast and oblique subduction and was characterized by important arc plutonism (the Peruvian Coastal Batholith) and formation of volcanosedimentary basins known as the Western Peruvian Trough (WPT). We present high-precision U–Pb ages and initial Hf isotopic compositions of zircon from conformable volcanic and crosscutting intrusive rocks within submarine volcanosedimentary strata of the WPT hosting the Perubar massive sulfide deposit. Zircons extracted from both the volcanic and intrusive rocks yield concordant U–Pb ages ranging from 67.89 ± 0.18 Ma to 69.71 ± 0.18 Ma, indicating that basin subsidence, submarine volcanism and plutonic activity occurred in close spatial and temporal relationship within the Andean magmatic arc during the Late Cretaceous. Field observations, satellite image interpretation, and plate reconstructions, suggest that dextral wrenching movements along crustal lineaments were related to oblique subduction. Wrench tectonics is therefore considered to be the trigger for the formation of the WPT as a series of pull-apart basins and for the emplacement of the Coastal Batholith. The zircon initial ϵ_{Hf} values of the dated magmatic rocks fall between 5.5 and 7.4, and indicate only very subordinate influence of a sedimentary or continental component. The absence of inherited cores in the zircons suggest a complete lack of old basement below the WPT, in agreement with previous U–Pb and Sr isotopic data for batholithic rocks emplaced in the WPT area. This is supported by the presence of a most likely continuous block of dense ($\sim$3.0 g/cm^3) material observed beneath the WPT area on gravimetric crustal cross sections. We suggest that this gravimetric anomaly may correspond to a piece of lithospheric mantle and/or oceanic crust inherited from a possible Late Permian–Triassic rifting. Such young and mafic crust was the most probable source for arc magmatism in the WPT area.

Keywords Andean magmatism · Continental arc · U–Pb dating · Hf isotopes · Strike-slip basins

M. Polliand · U. Schaltegger (✉) · L. Fontboté
Department of Mineralogy,
University of Geneva, Rue des Maraîchers 13,
1205 Geneve, Switzerland
E-mail: mpolliand@yahoo.fr
E-mail: urs.schaltegger@terre.unige.ch
Tel.: +41-22-3796638
Fax: +41-22-3793210
E-mail: lluis.fontbote@terre.unige.ch

U. Schaltegger · M. Frank
Department of Isotope Geology and Mineral Resources,
Federal Institute of Technology ETH,
Sonneggstrasse 5, 8092 Zurich, Switzerland
E-mail: martin.frank@erdw.ethz.ch

Introduction

During late-Early to Late Cretaceous the relative motion between the oceanic Farallon (previously Phoenix) and South American plates along the central Andean margin was characterized by a period of high convergence rate (e.g., Jaillard et al. 2000; Larson 1991; Soler and Bonhomme 1990) with a significant oblique component (northerly to north–northeasterly motion) of the subducted lithosphere (e.g., Jaillard 1994; Gordon and Jurdy 1986; Duncan and Hargraves 1984) and a most likely absolute trenchward motion of the South American plate (e.g., Jaillard and Soler 1996; Jaillard 1994; P. Soler, unpublished PhD thesis) due to the definitive opening of the South Atlantic ocean at about 110 Ma (e.g., Scotese et al. 1988; Larson and Pitman 1972). Along the coastal margin of Peru, this period of fast and oblique subduction was characterized by important arc magmatism and formation of volcanosedimentary basins with high average subsidence rates, known as the Mesozoic Western Peruvian Trough (WPT; e.g., Cobbing 1978; Atherton et al. 1983; Fig. 1a). The development of the WPT was accompanied and followed by

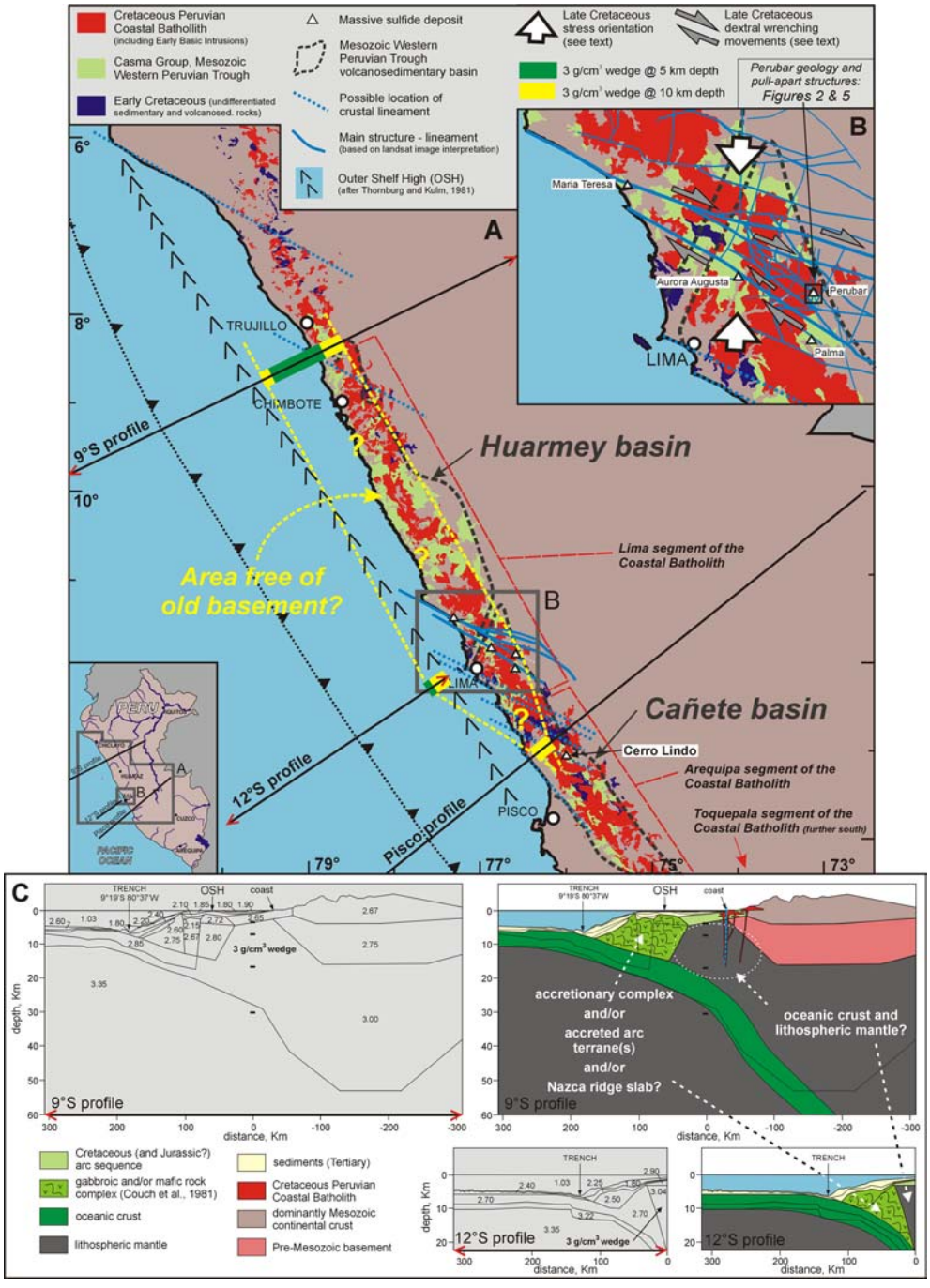

Fig. 1 **a** Geologic map of the Peruvian Coastal Batholith and Mesozoic Western Peruvian Trough (WPT) with related volcanosedimentary basins hosting massive sulfide deposits. Volcanosedimentary basin limits after Vidal (1987), Atherton et al. (1983), and Cobbing (1978). The *yellow doted lines* encompass the 3.0 g/cm^3 wedge at 10-km depth. Distribution of the Cretaceous Peruvian Costal Batholith, Casma Group, and Early Cretaceous strata after the digital version of the geological map of Peru (INGEMMET 2000). **b** Main lineaments and structures based on Landsat-5 TM image (*Red* Band 7; *Green* Band 4; *Blue* Band 2) interpretation, downloaded from http://www.zulu.ssc.nasa.gov/mrsid/. **c** Geologic interpretation of the deep sturctures along the 9°S and 12°S gravimetric, crustal and subcrustal cross sections (Couch et al. 1981; Jones 1981) of the continental margin of Peru

intrusion of numerous plutons that form the present-day Peruvian Coastal Batholith (Fig. 1), mostly emplaced between about 100 Ma and 30 Ma (e.g., Soler and Rotach-Toulhoat 1990a; Mukasa 1986a). Within the volcanosedimentary basins, several massive sulfide deposits were formed (i.e., Aurora Augusta, Cerro Lindo, Maria Teresa, Palma, Perubar; Fig. 1a, b), amongst which the Perubar deposit has been exploited from 1978 to 2000 and is the best studied (Polliand 2005; Polliand and Fontboté 2000; Vidal 1987).

The WPT in the central coastal margin of Peru, between about Trujillo and Pisco, has been subdivided into two major basin units known as the Huarmey and the Cañete basins (e.g., Atherton et al. 1983; Cobbing 1978; Fig. 1). According to several authors (e.g., Atherton and Aguirre 1992; Atherton and Webb 1989; Cobbing et al. 1981), both the Huarmey and Cañete basins had their main period of subsidence in the Albian, during which up to 9,000 m of volcanic (mainly basalt flows), volcaniclastic, and subordinate sedimentary rocks were deposited. These dominantly submarine volcanic and volcaniclastic successions have been attributed in the literature to the Casma Group and been described as Albian to Cenomanian in age (e.g., Atherton and Webb

1989; Cobbing et al. 1981). The extensional tectonic setting during which the Casma Group and related volcanosedimentary basins were formed was essentially attributed either to an extensional marginal basin with incipient formation of oceanic crust (e.g., Atherton and Aguirre 1992; Atherton 1990; Atherton and Webb 1989; Atherton et al. 1985), or to the extensional tectonic (pull-apart?) subsidence within the volcanic arc (e.g., Jaillard 1994; P. Soler, unpublished PhD thesis; Soler 1991). The overall geologic, lithologic and geometric framework of the WPT and related volcanosedimentary basins remains, however, poorly known, except in some areas near Huarmey and Culebras (Webb 1976; Myers 1980), and more detailed work is necessary to reach more sound geodynamic conclusions.

We present new U–Pb age determinations and initial Hf isotopic compositions of zircon from conformable volcanic and crosscutting intrusive rocks within submarine volcanosedimentary strata attributed so far to the Casma Group and hosting the Perubar massive sulfide deposit in the northeastern part of the Cañete basin (50 km east of Lima, 11°55′S 76°34′W; Fig. 1). These new data (1) demonstrate that the volcanosedimentary rocks of the Perubar area are much younger (Maastrichtian) than the Albian to Cenomanian age so far assumed for the Casma Group; (2) allow a better understanding of the temporal relationships between basin subsidence, subaqueous volcanism, hydrothermal massive sulfide mineralization, and plutonism during the uppermost Cretaceous in this region of the Peruvian Andes, (3) provide evidence for a formation of the WPT during extensional tectonic subsidence within the volcanic arc, and (4) constrain the melt sources and the nature of the basement beneath the central Peruvian coastal margin. Finally, this paper proposes a new hypothesis for the continental growth of the Peruvian active margin during late Early to Late Cretaceous, when the tangential component between the converging South American and Farallon plates was large.

Geologic setting of the volcanosedimentary rocks hosting the Perubar deposit

The Late Cretaceous volcanosedimentary strata that host the Perubar massive sulfide deposit are located in the northeastern part of the Cañete basin (Fig. 1a). These strata are truncated to the east and north by younger intrusions (i.e., the Canchacaylla monzogranite pluton and the Inclinado quartz monzodiorite porphyry stock, Fig. 2) and overlapped to the south by more recent continental volcanic deposits (i.e., the Calipuy Group, Fig. 2). The Canchacaylla monzogranite yields an hornblende K–Ar age of 66.7 ± 2 Ma (Vidal 1987). The smaller and moderately altered hornblende + plagioclase + biotite phenocryst-bearing Inclinado quartz monzodiorite porphyry (sample number 4 in Fig. 3a), that follows the north–south-trending Inclinado fault over a distance of 1,400 m (Fig. 2), yields a concordant zircon U–Pb age of 67.89 ± 0.18 Ma (Table 1). The Ricardo Palma tonalite, delimiting the western part of the basin (Fig. 2), is overlain by the volcanosedimentary strata and most probably constituted the western bedrock shoulder of the basin (Fig. 2). According to Vidal (1987) and Mukasa (1986a), the Ricardo Palma tonalite yields a 82.0 ± 2.3 Ma hornblende K–Ar age and concordant zircon U–Pb ages of 86.4 and 84.4 Ma, respectively. It was emplaced into older magmatic rocks of the Coastal Batholith and Early Cretaceous sedimentary strata such as those exposed further west of the study area along the coast line (Fig. 1a, b). Both the older and younger intrusions occurring in the Perubar area belong to the Cretaceous Peruvian Coastal Batholith.

The stratigraphy of the studied volcanosedimentary succession at Perubar has been divided into four main lithological units defined, from bottom to top, as the *Footwall, Prospective, Hangingwall* and *Upper Units*, respectively. Their lithological description is given in Fig. 3a. These volcanic and sedimentary strata were erupted and deposited in a pull-apart marine basin environment (Fig. 3b; Polliand 2005) without important periods of interrupted sedimentation, since less than 2 Ma separate the end of the *Footwall Unit* sedimentation and the deposition of the *Upper Unit* (Fig. 3a).

The *Hangingwall* and *Upper Unit* deposits (Fig. 3) are interpreted as the result of a tectonically controlled caldera collapse, where collapse and magmatic plumbing were influenced by pre-existing faults (Polliand 2005). The *Hangingwall Unit* polymictic breccias represent debris avalanche deposits resulting from a gravitational fault-block subsidence, that occurred prior to a catastrophic eruption responsible for the deposition of the *Upper Unit* pyroclastic and/or volcaniclastic debris flow deposits (Polliand 2005). The latter are inferred to be genetically related to the ignimbrite that outcrops along the Inclinado fault (Fig. 2), interpreted as the synvolcanic infill of a major eruptive fissure delineated by that same fault (Fig. 3b; Polliand 2005).

The massive sulfide mineralization, situated within the *Prospective Unit* (Fig. 3), was formed at the seafloor during a period of coeval submarine volcanism including the formation of lava domes, hyaloclastites, volcaniclastic sediments, and the sedimentation of impure limestones (Polliand 2005). The mineralizing hydrothermal event caused the strong hydrothermal alteration of the host and footwall rocks. A strongly hydrothermally altered, devitrified, perlitically and/or hydrothermally fractured, flow-banded rhyolite, showing relict feldspar crystals and situated in the upper portion of the *Lower Unit* (sample number 1 in Fig. 3a), and a strongly hydrothermally altered porphyritic rhyolite with plagioclase > quartz > K-feldspar (sample 2 in Fig. 3a) directly overlying the massive sulfide mineralization, yield zircon U–Pb concordant ages of 69.71 ± 0.18 Ma and 68.92 ± 0.16 Ma, respectively (Table 1 and Fig. 4). In addition, moderately altered aplites and rhyodacitic dykes with plagioclase > K-feldspar phenocrysts

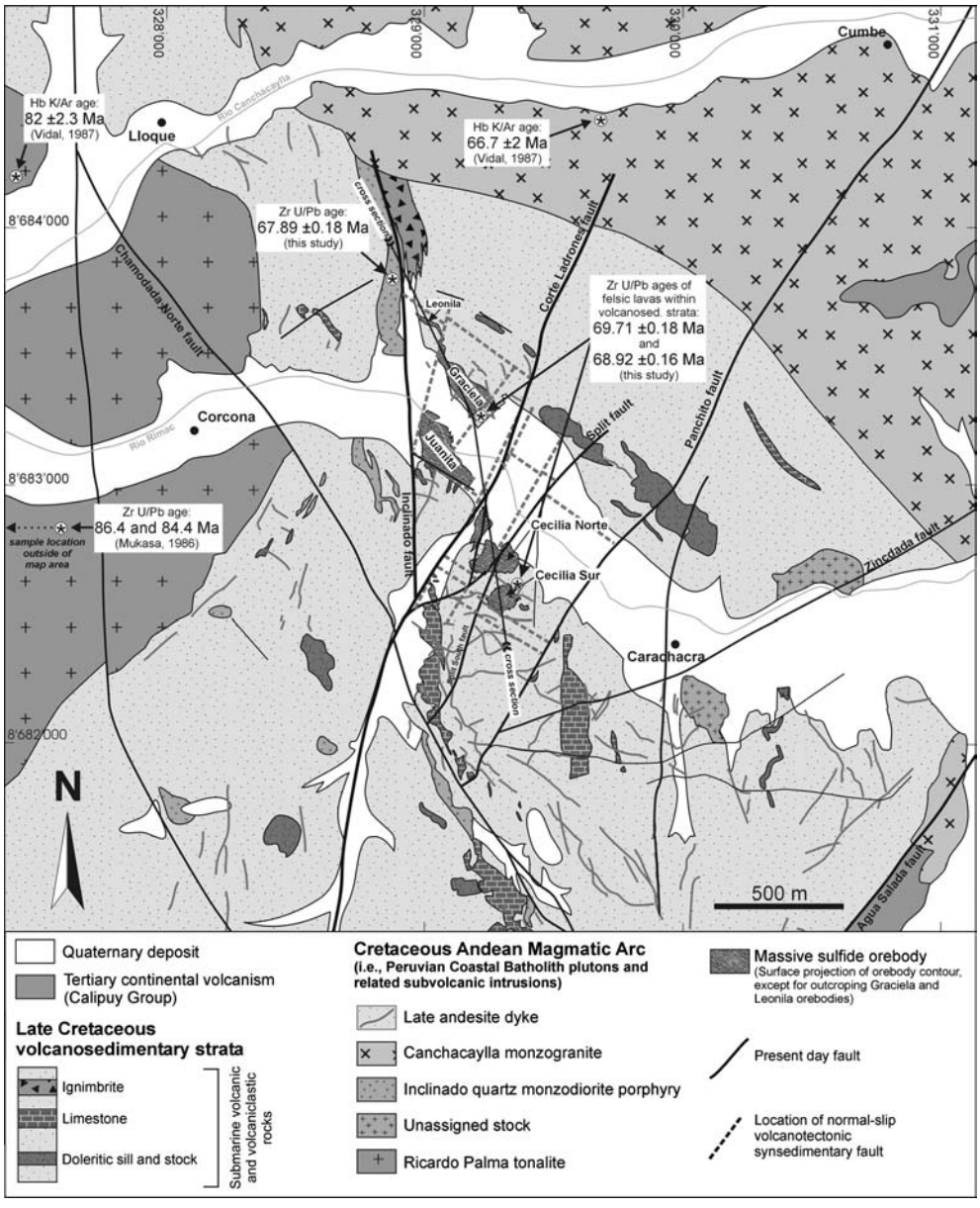

Fig. 2 Geologic map of the Perubar deposit area. See Fig. 3b for cross section. Coordinates are UTM

crosscut the *Footwall and Prospective Units* and possibly the whole stratigraphic column, although crosscutting relationships with the *Hangingwall* and *Upper Units* were not observable in the field (Fig. 3). One of these rhyodacitic dykes was dated and yields a concordant zircon U–Pb age of 67.94 ± 0.16 Ma (Table 1 and sample number 3 in Fig. 3a; Fig. 4).

U–Pb and Hf isotopic determinations

Determinations of U–Pb ages and analysis of initial Hf isotopic compositions in zircon were carried out on four different volcanic, subvolcanic and intrusive lithologies from the Perubar deposit area (see Figs. 3a, 4), consisting of: (1) a *flow-banded rhyolite* situated in the upper portion of the *Lower Unit*; (2) a massive *porphyritic rhyolitic lava*, directly overlying the massive sulfide orebodies and representing the upper limit of the *Hangingwall Unit*; (3) a *porphyritic rhyodacitic dyke*, believed to crosscut the whole stratigraphy; (4) the *Inclinado quartz monzodiorite porphyry*. U–Pb and Hf isotope data are summarized in Tables 1 and 2 (analytical techniques follow those in Schaltegger et al. 2002).

Flow-banded rhyolite (MPP657; Fig. 4a)

The zircons are transparent, mostly subhedral to prismatic, and have a uniform U concentration of 403–432 ppm. Three multigrain analysis (sample no. 1–3) yield reproducible concordant points that define a mean $^{206}Pb/^{238}U$ age of 69.71 ± 0.18 Ma (Fig. 4). Amongst

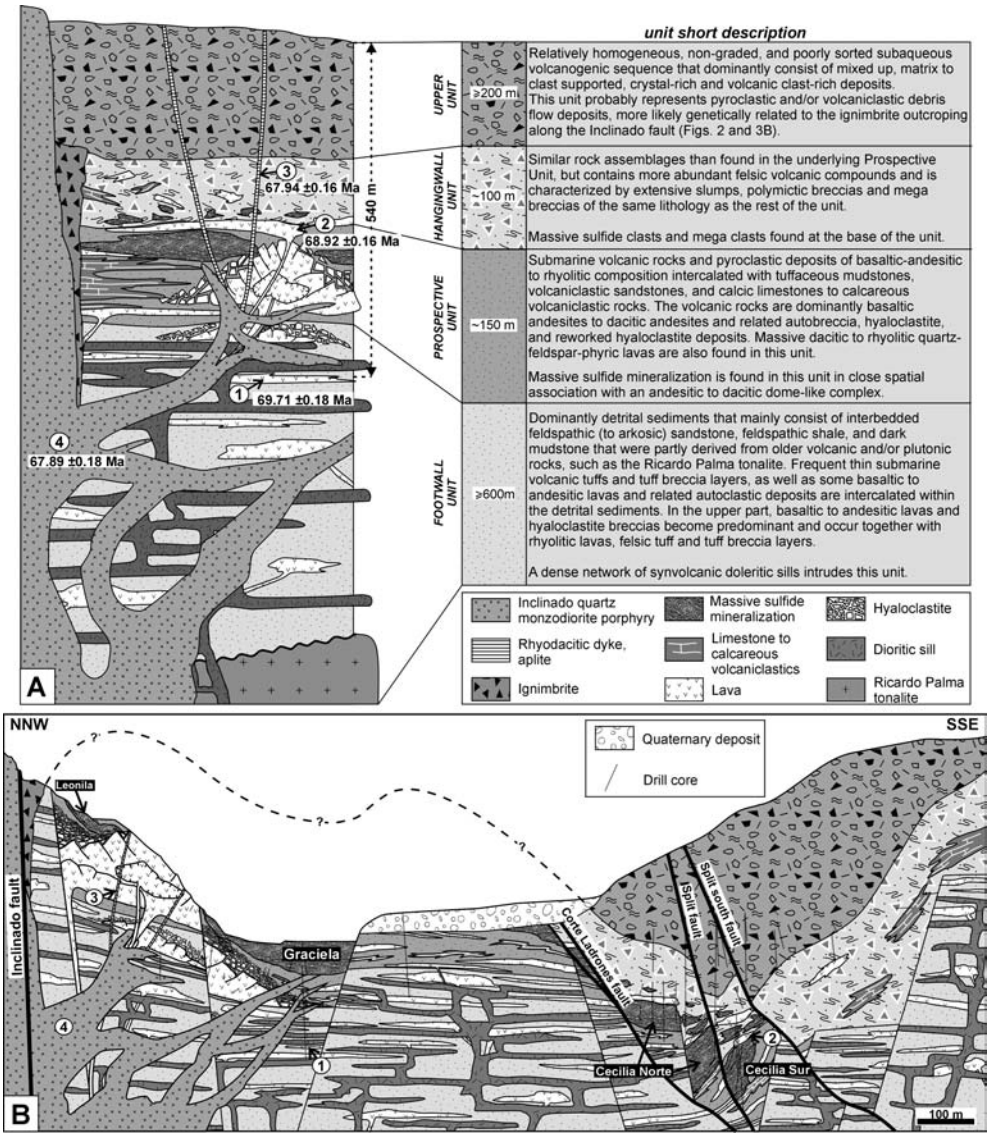

Fig. 3 **a** Lithostratigraphic column of the Late Cretaceous volcanosedimentary strata hosting the Perubar deposit. Numbers 1–4 delineate dated rock samples (see Table 1). **b** Longitudinal section across the Perubar VHMS deposit (see Fig. 2 for location). Note the deeply subsided blocks along the steep synsedimentary faults. This section was constructed on the basis of drill core, superficial, and underground working informations processed with the Gemcom mining software

these three multigrain fractions, Hf isotopic data were determined for two of them (1 and 2) and yield uniform initial ϵ_{Hf} of 7.4 ± 0.2 and 7.0 ± 0.3.

Porphyritic rhyolitic lava (MPP594; Fig. 4b)

The zircons of this rhyolite are transparent and most of them have a G-type euhedral morphology (according to Pupin 1980). The analysed fractions are U-rich, with relatively homogeneous concentrations ranging between 3,067 ppm and 3,244 ppm. Three multigrain analyses (no. 4–6) yield well reproducible $^{206}Pb/^{238}U$ ratios that define a mean age of 68.92 ± 0.16 Ma. The ϵ_{Hf} values for zircon fractions 5 and 6 are 5.7 ± 3.4 and 7.7 ± 0.5. The ϵ_{Hf} value measured for fraction 4 (i.e., 11.0 ± 1.3) is believed to represent an analytical outlier, since it strongly deviates from the other thirteen ϵ_{Hf} values centered around a value of 6 (Table 2).

Porphyritic rhyodacitic dyke (JG120; Fig. 4c)

The zircon population consists of one type of transparent euhedral grains, which mostly have a G-type morphology. About half of the zircons show small transparent melt inclusions; they have relatively uniform U concentrations ranging between 332 ppm and 593 ppm. Five multigrain fractions (no. 7–11) were analyzed and yield similar, reproducible $^{206}Pb/^{238}U$ ratios defining a concordant age of 67.94 ± 0.16 Ma. When removing the two analytical points 7 and 8, which yield significantly larger uncertainties due to their higher common lead concentrations, a mean concordant $^{206}Pb/^{238}U$ age of 67.91 ± 0.17 Ma can be calculated. Since these two ages are the same within error, the age calculated on the basis of the five analytical points (67.94 ± 0.16 Ma) will be preferred. The ϵ_{Hf} values obtained for all analyzed fractions are relatively uniform and fall between 5.5 ± 0.3 and 6.9 ± 0.5.

Table 1 U–Pb isotopic data

No.	Description	Weight (mg)	Number of grains	Concentrations				Atomic ratios							Apparent ages (Ma)			Error corr.
				U (ppm)	Pb rad (ppm)	Pb nonrad. (pg)	Th/U[a]	206/204[b]	206/238[c, d]	Error 2s (%)	207/235[c]	Error 2s (%)	207/206[c, d]	Error 2s (%)	206/238[d])	207/235	207/206[d]	
MPP657																		
1	Prism to subround	0.0076	6	432	5.05	2.6	0.62	876	0.01085	0.39	0.07101	0.91	0.04746	0.68	69.58	69.65	72.28	0.73
2	Subhedral	0.0036	6	419	4.86	2.9	0.57	372	0.01089	0.37	0.07148	1.49	0.04476	1.36	69.85	70.11	78.85	0.46
3	Subhedral	0.0024	7	403	4.88	1.0	0.74	684	0.01089	0.53	0.07129	1.51	0.04747	1.40	69.84	69.92	72.84	0.38
MPP594																		
4	G-types euh	0.0011	4	3151	39.26	0.8	0.92	2910	0.01076	0.39	0.07017	0.51	0.04732	0.36	68.96	68.86	65.31	0.71
5	G-types euh spr	0.0024	5	3244	40.93	0.5	0.96	11195	0.01074	0.38	0.07032	0.41	0.04748	0.20	68.87	69.01	73.60	0.87
6	Small abr	0.0032	4	3067	39.60	4.5	1.04	1494	0.01074	0.35	0.07048	0.51	0.07458	0.34	68.89	69.16	78.43	0.74
JG120																		
7	Clear euh	0.0081	6	332	3.98	11.0	0.74	182	0.01064	0.73	0.07016	2.38	0.04783	2.27	68.22	68.85	90.93	0.30
8	Round clrls	0.0028	6	403	4.63	2.2	0.78	357	0.01062	1.56	0.06890	2.64	0.04708	2.91	68.07	67.66	53.12	0.11
9	Round to prism	0.0036	5	593	7.07	1.3	0.79	1123	0.01058	0.41	0.06919	0.87	0.04742	0.75	67.86	67.93	70.56	0.51
10	Round	0.0040	5	465	5.40	0.6	0.68	2229	0.01059	0.47	0.06943	0.61	0.04759	0.46	67.94	68.16	75.84	0.67
11	Prism	0.0044	5	499	5.83	1.3	0.72	1,129	0.01059	0.34	0.06912	0.87	0.04733	0.75	67.92	67.86	65.83	0.52
MPP338																		
12	Round	0.0086	6	238	2.73	4.2	0.65	344	0.01057	0.40	0.06898	1.99	0.04739	1.84	67.78	67.73	65.78	0.46
13	spr	0.0046	5	328	3.98	0.7	0.87	1378	0.01059	0.43	0.06921	0.82	0.04741	0.70	67.89	67.95	69.77	0.52
14	Prism lge	0.0065	3	103	1.23	0.4	0.79	3444	0.01060	0.45	0.06946	0.65	0.04753	0.49	67.96	68.18	76.15	0.66

euh euhedral, *clrls* colourless, *incl* inclusions, *prism* prismatic, *spr* short-prismatic, *subh* subhedral, *transp* transparent, G-type zircons according to Pupin (1980); analyses 1–6 unabraded, 7–10 abraded

[a]Calculated on the basis of radiogenic $^{208}Pb/^{206}Pb$ ratios, assuming concordancy

[b]Corrected for fractionation and spike

[c]Corrected for fractionation (.09%), spike, blank and common lead (Stacey and Kramers 1975)

[d]Corrected for initial Th disequilibrium, using an estimated Th/U ratio of 4 for the melt

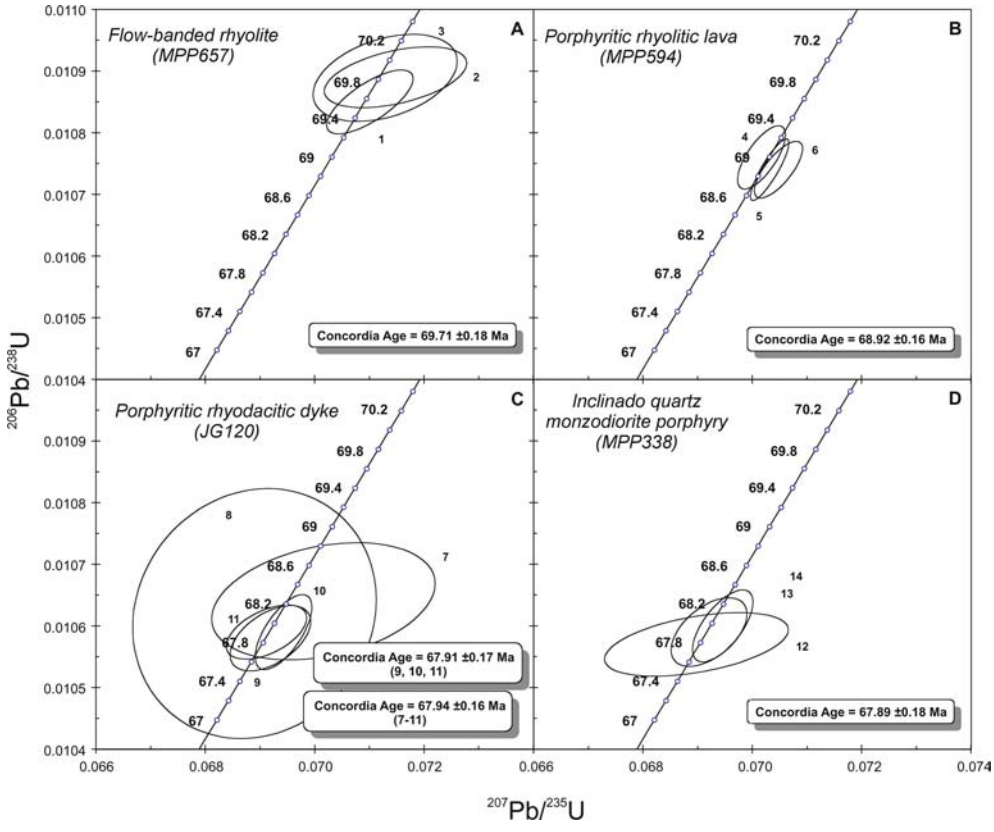

Fig. 4 U–Pb concordia diagrams for volcanic and intrusive lithologies at Perubar

Inclinado quartz monzodiorite porphyry (MPP338; Fig. 4d)

Two zircon populations are present in this rock, the first consisting of long prismatic transparent, the second of round to short-prismatic transparent grains. The short prismatic zircons have a U content of 238 and 328 ppm and the long prismatic of 103 ppm. Three multigrain analyses (no. 12–14) yield reproducible concordant points that define a mean $^{206}Pb/^{238}U$ age of 67.89 ± 0.18 Ma. The ϵ_{Hf} for the three analyzed fractions are relatively uniform and range between 5.9 ± 0.4 and 6.6 ± 0.5.

Tectonic setting

The main structural elements in the Perubar deposit area are dominantly N- to NNE- and NW-oriented synsedimentary and later reactivated faults (Figs. 2, 5). The synsedimentary faults can be recognized by changes of depositional facies (Fig. 3b; Polliand 2005). When removing Tertiary dextral normal-slip movements that occurred along the main Corte Ladrones and Split faults (Polliand 2005), the synsedimentary faults define a typical rhomb-shaped structure (Fig. 5), suggesting a pull-apart origin for the Perubar basin. At a regional scale, the Perubar deposit is situated between two major NW-oriented crustal lineaments (recognized on a Landsat-5 image) extending to the coast and being reflected in the orientation of the coastline (Fig. 1b). Similar structures are visible along the Peruvian coast from about 6° to 13°S (Fig. 1a). The strongly oblique northerly to north-northeasterly motion assumed for the subducting slab (Farallon plate) during Late Cretaceous times (e.g., Pardo-Casas and Molnar 1987; Gordon and Jurdy 1986; Duncan and Hargraves 1984), is in agreement with dextral wrenching movements along these NW-oriented crustal lineaments (Fig. 1b). They were also recognized and described in the ~100 Ma to ~63 Ma-old Haura plutonic complex north of Lima (Bussell 1983). The orientation and extensional direction of the pull-apart basin structure evidenced at Perubar are in full agreement with the large-scale structures (Figs. 1b, 5) and thus suggest that Late Cretaceous dextral wrench tectonics associated with oblique subduction may have generated the Perubar strike-slip basin and possibly the whole WPT.

Discussion of the U/Pb ages and Hf isotope data

Timing of plutonism and basin subsidence during the Late Cretaceous

Sedimentation in the Perubar pull-apart basin most likely started in the early Maastrichtian, before the 69.71 ± 0.18 Ma dated subaqueous flow-banded rhyolite was formed (no. 1, Fig. 3). The 10–15-Ma older Ricardo Palma tonalite (Fig. 2) is inferred to have formed the

Table 2 Hf isotopic data

Number	$^{176}Hf/^{177}Hf$ (0)	$^{176}Hf/^{177}Hf$ (T)[a]	±2s	ϵHf (T)[b]	±2s	T(DM) (Ga)[c]
MPP657						
1	0.282937	0.282930	6	7.4	0.2	0.63
2	0.282927	0.282920	9	7.0	0.3	0.65
3		–	–	–	–	–
MPP594						
4	0.283041	0.283035	36	(11.0)	1.3	0.41
5	0.282889	0.282883	94	5.7	3.4	0.73
6	0.282936	0.282940	14	7.7	0.5	0.61
JG120						
7	0.282883	0.282877	6	5.5	0.3	0.74
8	0.282887	0.282881	16	5.6	0.6	0.73
9	0.282923	0.282917	12	6.9	0.5	0.66
10	0.282908	0.282902	7	6.3	0.3	0.69
11		–	–	–	–	–
MPP338						
12	0.282905	0.282899	10	6.2	0.4	0.69
13	0.282895	0.282889	9	5.9	0.4	0.72
14	0.282915	0.282909	11	6.6	0.5	0.67

[a]The Hf fraction was isolated using Eichrom Ln-spec resin, and measured in static mode on a NuPlasma multi-collector ICP-MS using a MCN-6000 nebulizer for sample introduction. Zircons were corrected for in situ radiogenic ingrowth from ^{176} Lu using an estimated ^{176} Lu/^{177} Hf of 0.005. The Hf isotopic ratios were corrected for mass fractionation using a $^{179}Hf/^{177}Hf$ value of 0.7325 and normalized to $^{176}Hf/^{177}Hf$ = of 0.282160 of the JMC-475 standard (Blichert-Toft et al. 1997). Mean isotopic values are at the 95% confidence level

[b]Calculated with present-day CHUR values of $^{176}Hf/^{177}Hf$ = 0.282772, ^{176} Lu/^{177} Hf = 0.0332

[c]Calculated with present-day DM values of $^{176}Hf/^{177}Hf$ = 0.283252, ^{176} Lu/^{177} Hf = 0.04145 and a crustal ^{176} Lu/^{177} Hf = 0.017 (Blichert-Toft and Albarède 1997)

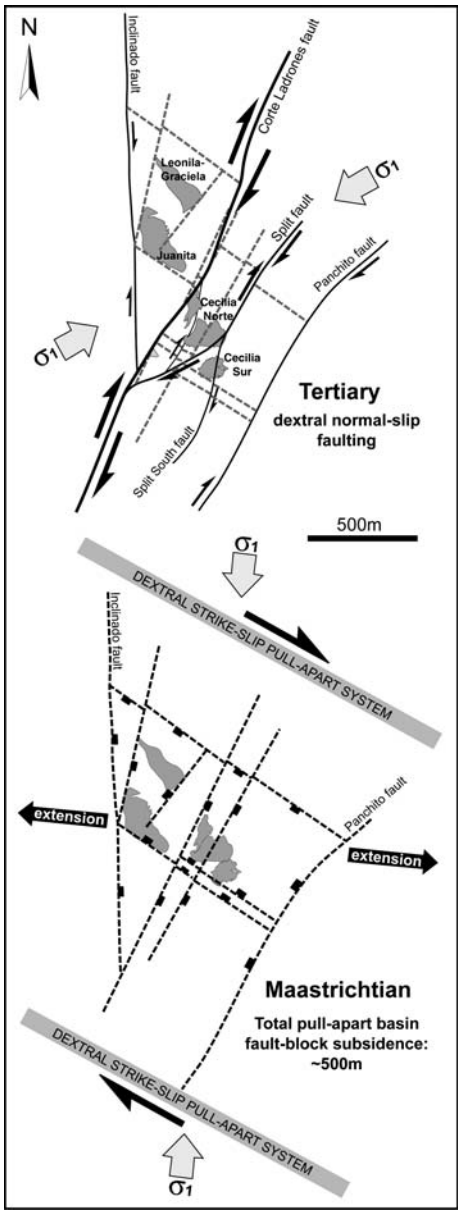

Fig. 5 Model for Late Cretaceous pull-apart origin of the Perubar basin. The tectonic stress (σ_1) is inferred from relative plate motion reconstructions between the South American continent and the oceanic Farallon plate (e.g., Gordon and Jurdy 1986; Duncan and Hargraves 1984)

bedrock and the western shoulder of this subsiding basin. The upper, 540-m thick, volcanosedimentary strata were deposited between 69.71 ± 0.18 Ma and 67.89 ± 0.18 Ma, ages that correspond to the flow-banded rhyolite and the Inclinado monzonite porphyry, respectively (no. 1 and 4, Fig. 3), yielding a minimum average sedimentation rate of 0.3 mm/year. The massive sulfide mineralization formed within the 0.8-Ma interval comprised between the 69.71 ± 0.18 Ma flow-banded rhyolite and the 68.92 ± 0.1 Ma porphyritic rhyolitic lava (no. 1 and 2, Fig. 3). Therefore, the studied volcanosedimentary strata in this part of the Cañete basin cannot be considered as a part of the Casma Group but represent a distinct and younger basin sedimentation event, since they were emplaced in the uppermost Cretaceous (Maastrichtian) instead of the mid-Cretaceous (Albian–Cenomanian) age previously defined for the Casma Group (Atherton and Webb 1989 and references therein).

The deposition of the studied volcanosedimentary pile and related massive sulfide deposit was quickly followed by the injection of porphyritic rhyodacitic dykes at 67.91 ± 0.17 Ma (no. 3, Fig. 3) and the intrusion of both the Inclinado porphyry and the Canchacaylla pluton at 67.89 ± 0.18 Ma (no. 4, Fig. 3) and 66.7 ± 2 Ma (Vidal 1987; Fig. 2), respectively. Since these two intrusive rocks belong to the subduction-related arc magmatism of the Peruvian Coastal Batholith (e.g., P. Soler, unpublished PhD thesis; Soler and Bonhomme 1990; Mukasa 1986a), it is likely that the subaqueously erupted volcanic deposits at Perubar represent the effusive counterpart of the plutonic arc. Therefore, Late Cretaceous intra-arc strike-slip faulting, as observed at Perubar (Figs. 3b, 5), was most probably responsible for pull-apart basin subsidence and related subaqueous volcanism, and provided at the same time space in the crust for the emplacement of plutons. This interpretation is in agreement with mechanisms related to oblique convergence, the latter being typically

resolved into a strongly orthogonal compressional component at the trench and a strike-slip component expressed by structures in the forearc and arc itself (Fitch 1972).

Melt sources—evidence for lacking Precambrian basement beneath the WPT

The ϵ_{Hf} values determined for the zircon fractions of the four different analyzed lithologies at Perubar all fall between 5.5 ± 0.3 and 7.7 ± 0.2 (Table 2). This range of positive values indicates only very subordinate contamination by a sedimentary or continental component during emplacement of both the volcanic and intrusive rocks at Perubar. The absence of inherited Proterozoic ages in the zircons measured in both the four dated samples at Perubar and in the Lima segment of the Coastal Batholith in general (Mukasa 1986a; Fig. 1a) indicates the lack of old basement beneath the WPT area. This contrasts with the occurrence of inherited zircons from the Precambrian basement of the Arequipa craton in plutons from the Arequipa and Toquepala segments of the Coastal Batholith (Mukasa 1986a; Fig. 1a). Moreover, the Coastal Batholith in the Lima segment displays consistent lead and strontium isotopic ratios ($^{206}Pb/^{204}Pb$: 18.554–20.803; $^{87}Sr/^{86}Sr$: 0.70307–0.70516), which infer that the rocks are apparently uncontaminated by upper crustal radiogenic components (e.g., Haeberlin 2004; Macfarlane et al. 1990; Soler and Rotach-Toulhoat 1990a, b; Mukasa 1986b) and thus suggest a lack of old basement below the WPT area between Pisco and Chimbote (Fig. 1a). It is supported by the presence of a most likely continuous block of dense (3.0 to 3.04 g/cm^3) material (oceanic crust and lithospheric mantle?) beneath the WPT area between Pisco and Trujillo according to the gravimetric crustal cross sections (Couch et al. 1981; Jones 1981) shown in Fig. 1a and c. At the latitude of the 12°S profile, we extended the limit of the 3.0 g/cm^3 gravity anomaly to the eastern boundary of the Cañete basin (Fig. 1a), since no evidence of significant upper-crustal contamination can be identified in the studied volcanic and plutonic rocks at Perubar. This zone, free of old basement underlying the WPT, would correspond to the lead province Ib defined in Macfarlane et al. (1990), the lead of which is believed to have been extracted from an enriched upper mantle reservoir. Similarly, Soler and Rotach-Toulhoat (1990a) suggested that the homogeneous strontium isotopic composition (~0.704) of the Coastal Batholith between Pisco and Chimbote is related to an undepleted mantle source (OIB-type or enriched sub-continental) that was contaminated by fluids derived from the subducting slab and associated subducted sediments. The range of ϵ_{Hf} values between +5.5 and +7.7 of the volcanic and intrusive rocks at Perubar are compatible with: (1) such an enriched upper mantle source reservoir, (2) with a depleted mantle contaminated by slab-derived fluids carrying Hf (Woodhead et al. 2001), or alternatively, (3) with a mixture of enriched mantle and reworked oceanic crust. Hf model ages evidence an average mantle extraction or residence age of 0.6-0.7 Ga.

Implications of a pull-apart origin for the volcanosedimentary basins of the WPT

Several authors (e.g., Atherton and Aguirre 1992; Atherton 1990; Atherton and Webb 1989; Atherton et al. 1985) consider the WPT as an aborted ocean floor extensional marginal basin that had its main period of extension and subsidence during the Albian. This model mainly relies on the interpretation of the gravimetric and seismic data along the 9°S, 12°S and Pisco crustal cross sections (Fig. 1a, c; Couch et al. 1981; Jones 1981), where the dense 3.0 g/cm^3 gravity anomaly is attributed to mantle-derived material that floored and filled up this Albian marginal basin. Accordingly, the 2.67–2.8 g/cm^3 blocks underlying the so-called "Outer Shelf High"area (Fig. 1a, c) are interpreted as pieces of rifted continental crust.

However, we have demonstrated that the Albian marginal basin model cannot be applied to the volcanosedimentary strata exposed at Perubar, the latter being Maastrichtian in age and deposited within a pull-apart basin formed atop of the plutonic arc and related to the N to NNE motion assumed for the paleo-Pacific slab during Late Cretaceous times. Since a roughly northward motion of the subducting paleo-Pacific plate beneath the central Peruvian margin is also assumed for the preceeding Albian to Campanian period (e.g., Jaillard 2000; Jaillard 1994; Duncan and Hargraves 1984) combined with a high convergence rate (> 10 cm/year; Jaillard and Soler 1996; Larson 1991), we suggest that wrench tectonics, strike-slip faulting and subsequent pull-apart basin formation also occurred at that time, in line with the proposition of Jaillard (1994) and P. Soler (unpublished PhD thesis, Soler 1991) that the Casma Group-hosting volcanosedimentary basins possibly relate to extensional pull-apart subsidence within the volcanic arc. Thus, the WPT volcanosedimentary basins might represent distinct intra-arc pull-apart basin generations progressively migrating eastward with the arc from Albian to Maastrichtian times. During the Albian–Campanian period, the relative age of the subducted lithosphere was rapidly decreasing (e.g., Jaillard and Soler 1996; Jaillard 1994; Soler and Bonhomme 1990), leading most likely to a decrease of the slab dip. This was possibly coupled to an absolute trenchward motion of the overriding South American plate (e.g., Jaillard and Soler 1996; Soler and Bonhomme 1990). Both phenomena could account for the eastward migration of the arc.

The inferred intra-arc extensional pull-apart origin for the WPT volcanosedimentary basins implies a pre-late Early Cretaceous origin for the underlying dense 3.0 g/cm^3 structure (Fig. 1a, c). This 10 km thick block of dense material might represent a piece of lithospheric mantle

and/or oceanic crust inherited from a possible Late Permian–Triassic rifting, believed to have developed in the Eastern Cordillera of Peru and extended into Bolivia in the Late Triassic–Middle Jurassic (Sempere et al. 2002 and references therein). Several authors (e.g., Haeberlin 2004; Ramos and Aleman 2000; Dalziel et al. 1994) suggested that this rifting event would have removed the northwest prolongation of the Arequipa craton of southern Peru, from which the detached slice or slices are thought to have migrated northwards and possibly represent the allochthonous Oaxaquia Terrane in Mexico. The Outer Shelf High, which, in this case, cannot be considered as a piece of rifted continental crust, may therefore be interpreted as an accretionary complex and/or an accreted oceanic plateau (Nazca ridge?) and/or accreted island arc terranes previously formed on the paleo-Pacific plate (Fig. 1c). However, more work needs to be done prior to reach any firm conclusions on the origin and nature of the present-day deep structures found along the coastal margin of Peru between ~7°S and ~14°S.

The correlation between oblique subduction, basin formation and magmatism

The apparent correlation between plutonism, oblique subduction and associated strike-slip faulting observed in the study area suggest that the Cretaceous Peruvian Coastal Batholith might be related to episode(s) of oblique subduction, as already observed by Glazner (1991) for major episodes of Mesozoic plutonism in California. According to this author, major episodes of continental growth by addition of plutons to continental margins may occur only if there is a significant oblique component at the trench, the magmatic room problem being solved by passive emplacement of plutons at releasing bends in the strike-slip faults and conservation of volume by thrusting at the trench. Therefore, the central Peruvian continental margin may have built its own new crust (i.e. the Peruvian Coastal Batholith), by similar processes with magma originating from an enriched mantle source.

Numerous modern intra-arc fault-bounded basin analogues are observed in strike-slip zones related to oblique subduction, such as the Taupo volcanic zone in the Kermadec-Tonga intraoceanic arc (Cole and Lewis 1981), the Lake Managua pull-apart graben in the Nicaraguan Depression (Burkart and Self 1985), basins along the central Aleutian Ridge arc platform (Geist and Scholl 1992), and intra-arc depocenters along the central Salomon Trough (Ryan and Coleman 1992).

Conclusions

Basin subsidence, submarine volcanism and plutonic activity occurred in close spatial and temporal relationship within the Andean magmatic arc during the uppermost Cretaceous oblique subduction, indicating that wrench tectonics was the trigger of pull-apart basin formation and magmatism. The example of the Perubar basin evolution, during which volcanic activity progressively increased to reach a tectonically controlled submarine caldera collapse stage that was quickly followed by the intrusion of porphyries and plutons, fully supports this interpretation.

The zircon U–Pb ages of both volcanic and intrusive rocks at Perubar range between 67.89 ± 0.18 Ma and 69.71 ± 0.18 Ma, indicating that volcanosedimentary rocks of at least part of the Casma Group are not Albian–Cenomanian in age but were in fact formed during Maastrichtian times. The Perubar volcanic-hosted massive sulfide deposit was formed during Maastrichtian times, between 69.71 ± 0.18 Ma and 68.92 ± 0.16 Ma. Volcanic-hosted massive sulfide (VHMS) deposits in the Peruvian segment of the Andes, such as the Perubar deposit, are generally located along the major NW-oriented crustal lineaments, where contemporaneous strike-slip faulting, pull-apart basin opening, and magma plumbing were most probably acting. These structures are likely to represent old inherited deep crustal discontinuities, e.g., transform faults from a Late Permian–Triassic rifting event.

The initial ϵ_{Hf} values of the magmatic rocks fall between values of $+5.5$ and $+7.4$, and record subordinate contamination by a low-radiogenic Hf, possibly derived from slab sediments. These values may also represent an enriched mantle source and/or recycled oceanic crust as possible melt sources. The lack of inherited cores in zircons demonstrates that there is no old basement involved in the generation of volcanic and intrusive rocks at Perubar. We think that the data evidence the lack of old basement under the WPT, such as the Precambrian Arequipa massif in southern Peru (Wasteneys et al. 1995). Young and mafic crust is the probable source for the arc magmatism within the Lima segment of the Coastal Batholith. Voluminous plutonism in an arc environment thus requires extension of relatively hot crust triggering remelting and emplacement in pull-apart structures. This process is suggested to be equally important in oceanic arcs (such as the Kohistan Arc complex; Schaltegger et al. 2002) as well as in continental active margin situations such as in the Andes.

Acknowledgements This research was supported by the Swiss National Science Foundation grants FN 2000–54150.98 and FN 20–62000.00, and is part of a PhD thesis of the first author at the University of Geneva. We gratefully acknowledge W. Mueller and L. Oldham who instigated this project and transmitted us their knowledge of the Perubar deposit area, the geologists and staff of the Perubar mine for their help during the field work periods, especially R. Egoavil and C. Zumarán, and the geologists from Glencore Peru, M. Steinmann and S. Bureau, for logistical support during the project.

References

Atherton MP (1990) The Coastal Batholith of Peru; the product of rapid recycling of "new" crust formed within rifted continental margin. Geol J 25:337–349

Atherton MP, Aguirre L (1992) Thermal and geotectonic setting of Cretaceous volcanic rocks near Ica, Peru, in relation to Andean crustal thinning. J S Am Earth Sci 5:47–69
Atherton MP, Webb S (1989) Volcanic facies, structure, and geochemistry of the marginal basin rocks of central Peru. J S Am Earth Sci 2:241–261
Atherton MP, Pitcher WS, Warden V (1983) The Mesozoic marginal basin of central Peru. Nature 305:303–306
Atherton MP, Warden V, Sanderson LM (1985) The Mesozoic marginal basin of Central Peru: a geochemical study of within-plate-edge volcanism. In: Pitcher WS, Atherton MP, Cobbing EJ, Beckinsale RD (eds) Magmatism at a plate edge; the Peruvian Andes. Blackie, Glasgow, pp 47–58
Blichert-Toft J, Albarède F (1997) The Lu–Hf isotope geochemistry of chondrites and the evolution of the mantle-crust system. Earth Planet Sci Let 148:243–258
Blichert-Toft J, Chauvel C, Albarède F (1997) Separation of Hf and Lu for high-precision isotope analysis of rock samples by magnetic sector-multiple collector ICP-MS. Contrib Mineral Petrol 127:248–260
Burkart B, Self S (1985) Extension and rotation of crustal blocks in northern Central America and effect on the volcanic arc. Geology 13:22–26
Bussell MA (1983) Timing of tectonic and magmatic events in the Central Andes of Peru. J Geol Soc Lond 140:279–286
Cobbing EJ (1978) The Andean Geosyncline in Peru, and its distinction from Alpine geosynclines. J Geol Soc Lond 135:207–218
Cobbing EJ, Pitcher WS, Wilson JJ, Baldock JW, Taylor WP, McCourt W, Snelling NJ (1981) The geology of the Western Cordillera of northern Peru. Overseas Mem Inst Geol Sci, vol 5, pp 143
Cole JW, Lewis KB (1981) Evolution of the Taupo-Hikurangi subduction system. Tectonophysics 72:1–21
Couch RW, Whitsett RM, Huehn B, Briceno GL (1981) Structures of the continental margin of Peru and Chile. Geol Soc Am Mem 154:703–726
Dalziel IWD, Dalla Salda L, Gahagan LM (1994) Paleozoic Laurentia–Gondwana interaction and the origin of the Appalachian–Andean mountain system. Geol Soc Am Bull 106:243–252
Duncan RA, Hargraves RB (1984) Plate tectonic evolution of the Caribbean region in the mantle reference frame. Geol Soc Am Mem 162:81–93
Fitch TJ (1972) Plate convergence, transcurrent faults, and internal deformation adjacent to southeast Asia and the Western Pacific. J Geophys Res 77:4432–4460
Geist EL, Scholl DW (1992) Application of continuum models to deformation of the Aleutian island arc. J Geophys Res 97:4953–4967
Glazner AF (1991) Plutonism, oblique subduction, and continental growth; an example from the Mesozoic of California. Geology 19:784–786
Gordon RG, Jurdy DM (1986) Cenozoic global plate motions. J Geophys Res 91:12,389–12,406
Haeberlin Y, Moritz M, Fontboté L, Cosca M (2004) Carboniferous orogenic gold deposits at Pataz, Eastern Andean Cordillera, Peru: geological and structural framework, paragenesis, alteration, and $^{40}Ar/^{39}Ar$ geochronology. Econ Geol 99:73–112
INGEMMET (2000) Mapa geológico digitalizado del Perú (Escala 1:1'000'000). Lima, Instituto Geológico Minero y Metalúrgico, CD-ROM
Jaillard E (1994) Kimmeridgian to Paleocene tectonic and geodynamic evolution of the Peruvian (and Ecuadorian) margin. In: Salfity JA (ed) Cretaceous tectonics of the Andes. Earth evolution sciences monograph series. Wiesbaden, Vieweg, pp 101–167
Jaillard E, Soler P (1996) Cretaceous to early Paleogene tectonic evolution of the northern Central Andes (0–18 degrees S) and its relations to geodynamics. Tectonophysics 259:41–53
Jaillard E, Hérail G, Monfret T, Diaz-Martínez E, Baby P, Lavenu A, Dumon JF (2000) Tectonic evolution of the Andes of Ecuador, Peru, Bolivia and northernmost Chile. In: Cordani UG, Milani EJ, Thomaz Fihlo A, Campos DA (eds) Tectonic evolution of South America. In: 31st international geological congress, Rio de Janeiro, pp 481–559
Jones PR (1981) Crustal structures of the Peru continental margin and adjacent Nazca Plate, 9 degrees S latitude. Geol Soc Am Mem 154:423–443
Larson RL (1991) Latest pulse of Earth; evidence for a Mid-Cretaceous super plume. Geology 19:547–550
Larson RL, Pitman WC (1972) World-wide correlation of Mesozoic magnetic anomalies, and its implications. Geol Soc Am Bull 83:3645–3661
Macfarlane AW, Marcet P, LeHuray AP, Petersen U (1990) Lead isotope provinces of the Central Andes inferred from ores and crustal rocks. Econ Geol 85:1857–1880
Mukasa SB (1986a) Zircon U-Pb ages of super-units in the Coastal Batholith, Peru; implications for magmatic and tectonic processes. Geol Soc Am Bull 97:241–254
Mukasa SB (1986b) Common Pb isotopic compositions of the Lima, Arequipa and Toquepala segments in the Coastal Batholith, Peru; implications for magmagenesis. Geochim Cosmochim Acta 50:771–782
Myers JS (1980) Geologia de los cuadrangulos de Huarmey y Huayllapampa; hojas 21-g y 21 h, vol 33. Instituto Geologico Minero y Metalurgico, Lima, Peru, pp 153
Pardo-Casas F, Molnar P (1987) Relative motion of the Nazca (Farallon) and South American plates since Late Cretaceous time. Tectonics 6:233–248
Polliand M (2005) Genesis, evolution, and tectonic setting of the Upper Cretaceous Perubar Ba-Pb–Zn volcanic-hosted massive sulfide deposit. Terre and Environement, Thesis 3404, Section des Sciences de la Terre, Université de Genève, (in press)
Polliand M, Fontboté L (2000) The Perubar Ba-Pb-Zn VHMS deposit, Central Peru. In: Sherlock RL, Logan MAV (eds) VMS deposits of Latin America. Geological Association of Canada, Mineral Deposits Division, Special Paper, Vancouver 2:439–446
Pupin JP (1980) Zircon and granite petrology. Contrib Mineral Petrol 73:207–220
Ramos VA, Aleman A (2000) Tectonic evolution of the Andes. In: Cordani UG, Milani EJ, Thomaz Fihlo A, Campos DA (eds) Tectonic evolution of South America. In: 31st international geological congress, Rio de Janeiro, pp 635–685
Ryan HF, Coleman PJ (1992) Composite transform-convergent plate boundaries; description and discussion. Mar Petrol Geol 9:89–97
Schaltegger U, Zeilinger G, Frank M, Burg JP (2002) Multiple mantle source during island arc magmatism: U–Pb and Hf isotopic evidence from the Kohistan arc complex, Pakistan. Terra Nova 14:461–468
Scotese CR, Gahagan LM, Larson RL (1988) Plate tectonic reconstructions of the Cretaceous and Cenozoic ocean basins. Tectonophysics 155:27–48
Sempere T, Carlier G, Soler P, Fornari M, Carlotto V, Jacay J, Arispe O, Neraudeau D, Cardenas J, Rosas S, Jimenez N (2002) Late Permian–Middle Jurassic lithospheric thinning in Peru and Bolivia, and its bearing on Andean-age tectonics. Tectonophysics 345:153–181
Soler P (1991) El volcanismo Casma del Perú Central: cuenca marginal abortada o simple arco volcanico?. VII Congreso Peruano de Geología, Resúmenes Extendidos, Soc Geol Peru, Lima 2, pp 659–663
Soler P, Bonhomme MG (1990) Relation of magmatic activity to plate dynamics in central Peru from Late Cretaceous to present. Geol Soc Am Spec Pap 241:173–192
Soler P, Rotach-Toulhoat N (1990a) Implications of the time-dependent evolution of Pb- and Sr-isotopic compositions of Cretaceous and Cenozoic granitoids from the coastal region and the lower Pacific slope of the Andes of central Peru. Geol Soc Am Spec Pap 241:161–172
Soler P, Rotach-Toulhoat N (1990b) Sr-Nd isotope compositions of Cenozoic granitoids along a traverse of the central Peruvian Andes. Geol J 25:351–358

Stacey JS, Kramers JD (1975) Approximation of terrestrial lead isotope evolution by a two-stage model. Earth Planet Sci Lett 26:207–221

Thornburg TM, Kulm LD (1981) Sedimentary basins of the Peru continental margin; structure, stratigraphy, and Cenozoic tectonics from 6 degrees S to 16 degrees S latitude. Geol Soc Am Mem 154:393–422

Vidal CCE (1987) Kuroko-type deposits in the Middle-Cretaceous marginal basin of central Peru. Econ Geol 82:1409–1430

Wasteneys HA, Clark AH, Farrar E, Langridge RJ (1995) Grenvillian granulite-facies metamorphism in the Arequipa Massif, Peru; a Laurentia-Gondwana link. Earth Planet Sci Let 132:63–73

Webb SE (1976) The volcanic envelope of the coastal batholith in Lima and Ancash, Peru. PhD thesis, University of Liverpool

Woodhead JD, Hergt JM, Davidson P, Eggins SM (2001) Hafnium isotope evidence for ''conservative'' element mobility during subduction zone processes. Earth Planet Sci Let 192:331–346